AIAA AVIATION Forum
June 27-July 1, 2022, Chicago, IL & Virtual
AIAA AVIATION 2022 Forum

10.2514/6.2022-3936

Free-Size Optimization of a Stiffened Panel Using Equivalent Radiated Power

Luke Crispo[1], Wesley Dossett[2], Adam McKenzie[3], and Il Yong Kim[4]
Queen's University, Kingston, Ontario, K7L 3N6, Canada

Acoustic performance is not typically considered during the structural design of an aircraft fuselage, however the noise transmitted by the fuselage during flight can contribute to passenger discomfort. Structural-acoustic optimization approaches have been presented in research, but there is limited implementation in commercial design optimization software. This work investigates equivalent radiated power optimization in Altair OptiStruct as a means of indirectly minimizing radiated sound power over a broadband frequency range. Radiated sound power theory is reviewed and a methodology is presented for free-size optimization for equivalent radiated power. The proposed approach is applied to the design of chemical-milled pockets of a stiffened panel, ultimately achieving a small reduction in sound power compared to five other pocket designs. Further exploration is needed to conclude if equivalent radiated power optimization can achieve a meaningful reduction in sound power.

I. Introduction

Aircraft structural design traditionally focuses on objectives such as mass, stiffness, failure criteria, and cost to produce a structure that is lightweight, cost-effective, and supports major loads. In addition to its structural behaviour, an aircraft fuselage also transmits major sources of airborne and structure-borne noise to the cabin interior [1], which can contribute to passenger annoyance and discomfort [2] as well as impact flight staff health and performance [3]. Despite this, aircraft cabin noise is often a secondary design objective that is addressed after the airframe has been finalized, typically through added damping material or active methods, detailed extensively by Mixson and Powell [1] and by Wilby [4].

Design optimization tools, such as topology, size, and shape optimization, determine optimal design variable values to minimize an objective function subject to specified constraints. These tools have seen significant application in the aerospace field mainly focused on structural and aerodynamic design, with Sobieszczanski-Sobieski surveying developments in multidisciplinary aerospace design optimization [5] and Zhu et al. summarizing topology optimization research in aircraft design [6]. Examples of applications of topology optimization in the aerospace industry include the design of an aircraft seat using carbon composites [7], the design of a morphing serpentine engine inlet [8], and the design of a personal aerial vehicle [9].

Structural-acoustic optimization, summarized by Marburg [10], aims to use design optimization techniques to passively reduce radiated noise by changing a structure's geometry. Lamancusa developed a size optimization technique that was applied to the acoustic design of a rectangular panel, using different optimization objectives, including radiated sound power, mean square velocity, and radiation efficiency, all over a frequency range [11]. Cunefare et al. minimized radiated sound power using size optimization in a stiffened cylinder subject to a tonal excitation [12]. Du and Olhoff minimized radiated power in a flat plate and cylinder models using bi-material topology optimization [13]. Despite these research advances, there is limited implementation of structural-acoustic optimization methodologies into commercial design optimization software. Current approaches focus instead on natural frequency to indirectly minimize radiated noise in aircraft components, such as a stiffened bulkhead [14] or an engine support frame [15]. Equivalent radiated power (ERP) is another possible objective in Altair OptiStruct [16], and has been used as an objective function for topography optimization of an air conditioning enclosure panel [17].

[1] PhD Candidate, Department of Mechanical and Materials Engineering.
[2] MASc Student, Department of Mechanical and Materials Engineering.
[3] MASc Student, Department of Mechanical and Materials Engineering.
[4] Professor, Department of Mechanical and Materials Engineering.

The goal of this research is to optimize the structural design of a flat stiffened panel for acoustic performance using the existing design tools available in Altair OptiStruct. This paper will focus on ERP, outlining its relationship to radiated sound power and presenting a free-size optimization methodology. The approach will be applied to the design of chemical-milled pockets in a stiffened panel to minimize noise over a broadband frequency range. The optimized design generated by the methodology will be compared to other pocket designs in terms of radiated sound power to assess the performance and feasibility of using ERP optimization to improve acoustic performance.

II. Methodology

A. Calculation of ERP and Radiated Sound Power

The radiated sound power of a vibrating source can be estimated using the ERP calculation [18], which assumes the vibrating surface is acting as a piston with a mean square vibration velocity [19]. ERP calculation in finite element analysis uses results from the frequency response analysis of the structure, enabling significant computational advantages compared to a sound power calculation [20], which requires an acoustic mesh or numerical integration using the Rayleigh integral. OptiStruct calculates ERP as

$$ERP = \frac{1}{2}\eta_{rad}\rho_0 c\sum_j A_j v_j^2 \tag{1}$$

where v_j is the normal velocity and A_j is the associated area of the *j*-th node, which are summed over the entire radiated surface and multiplied by the speed of sound c, the density of air ρ_0, and a radiation loss factor η_{rad} (which is typically determined through experimental validation but is set equal to one in this analysis). While ERP is a simple method to estimate sound power from a structural frequency response analysis, it has some limitations that must be acknowledged:

1) It assumes far-field radiation;
2) It ignores acoustic short circuits (also known as cancellation and reinforcement effects); and
3) It ignores the impact of the acoustic fluid on the vibrating surface (if the acoustic fluid is not modelled).

Despite these known limitations, ERP represents an objective function of interest for design optimization, and further investigation is needed to determine if minimizing ERP (or input power) of a vibrating surface will have a net positive effect on radiated sound power.

Radiated sound power is calculated by integrating far-field intensity over a hemispherical surface centered on the vibrating surface. In OptiStruct, the hemispherical surface is meshed with microphone elements and acoustic pressure is calculated using the Rayleigh Integral equation

$$p_{jm} = \frac{f\rho_0 q}{r_{jm}} v_j i e^{-ikr_{jm}} \tag{2}$$

where p_{jm} is the acoustic pressure at the *m*-th microphone node due to the *j*-th source node, f is the frequency of the sound wave, q is a scaling factor, r_{jm} is the distance from the respective microphone to source node, and k is the acoustic wavenumber ($k = 2\pi f / c$). OptiStruct outputs a radiated sound power response calculated as

$$P_m^{Opti} = \sum_j \mathrm{Re}\left(p_{jm} p_{jm}^*\right) \tag{3}$$

where P_m^{Opti} is the OptiStruct power output at the *m*-th microphone node due to all source nodes and p_{jm}^* is the complex conjugate of p_{jm}. Note that this OptiStruct sound power output is not a true radiated sound power and must be modified as per Eq. (4) in a post processing calculation to match the theoretical equation for radiated sound power [19], where A_m is the area associated with the *m*-th microphone node.

$$P = \frac{1}{2\rho_0 c}\sum_m P_m^{Opti} A_m \tag{4}$$

This equation sums the adjusted radiated sound power for all microphone nodes. This sound power calculation using the Rayleigh integral still assumes far-field radiation and this analysis ignores the impact of the acoustic fluid, however it does account for acoustic short circuits. Therefore, these calculations will be used to validate if the ERP reductions measured during optimization translate to a meaningful reduction in sound power.

B. Stiffened Panel Model

A 1.5 m x 1.0 m flat rectangular skin panel stiffened with seven L-shaped stringers and four C-shaped frames was used as a test case for the ERP optimization methodology. The geometry was modeled in Altair HyperWorks using 37,502 shell elements with an average element size of 8mm. All components were modelled using Aluminum 2024 with the thicknesses and material properties specified in Table 1. Offset surfaces were connected using rivets represented with RBE3-CBUSH-RBE3 elements. Rivet properties were calculated assuming a 4.5 mm diameter and aluminum material properties using the Douglas fastener model [21], resulting in an axial stiffness of 412 kN/mm and shear stiffness of 33 kN/mm. A 6.86 m radius hemisphere centered on the panel was meshed using 2866 microphone elements for the radiated sound power analysis.

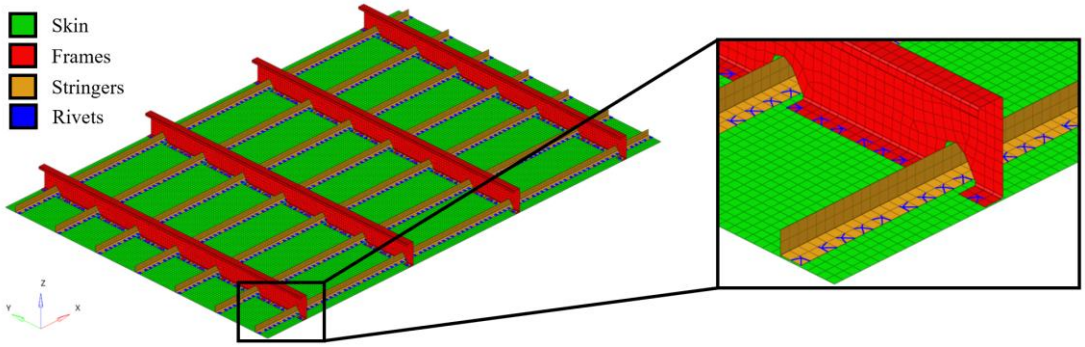

Fig. 1 Finite element model of a generic stiffened skin panel.

Table 1: Thickness and material properties of stiffened panel components

Component	Thickness [mm]	Material	Young's Modulus [GPa]	Poisson's Ratio	Density [g/cm^3]
Skin	2.032	Al 2024	72.4	0.33	2.77
Stringers	1.524				
Frames	0.9906				

The panel was pinned (constrained in all translational degrees of freedom) on all outer edges and unit loads were applied in separate steps perpendicularly to the skin. Fig. 2 depicts the applied loads and boundary conditions for the ERP optimization as well as the sound power analysis (used for verification). ERP optimization was conducted with 24 loads distributed across a quarter of a single bay (the area between two stringers and two frames) to provide an even distribution of loads across the surface without a large computational cost. Note that this loading does not favour a particular location on the panel because of the symmetry and pattern repetition constraints applied to the design variables, as discussed in the following section. Sound power analysis was conducted using 100 randomly placed loads across the center bay of the panel, following a rain-on-the-roof (or Monte-Carlo) loading method [22]. Both scenarios were solved for a broadband frequency range with excitations from 20 Hz to 1500 Hz in 200 logarithmically distributed steps.

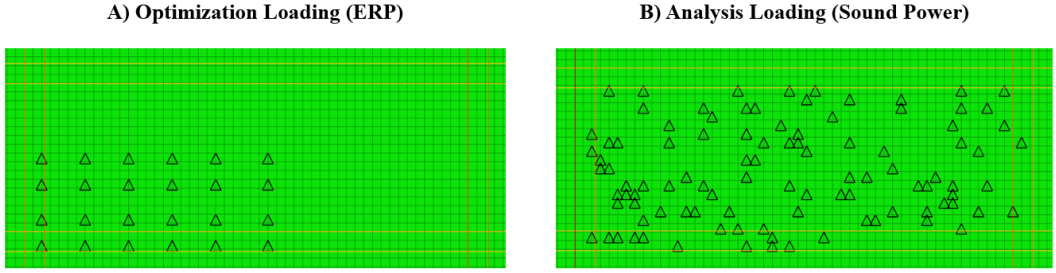

Fig. 2 Loading for stiffened panel model for A) optimization model and B) analysis model. Black triangles representing unit loads in the +z direction (applied in separate load steps). A single bay in shown with transparent stringers and frames.

C. Free-Size Optimization

Free-size optimization was implemented to determine the optimal thickness of all skin elements in the stiffened panel, represented by design variable vector $\underset{\sim}{x}$, with element thickness ranges between 1.270 mm to 2.032 mm (0.05" to 0.08"). The optimization problem statement in Eq. (5) minimizes the sum of ERP over the entire plate for the n applied unit loads over the ω frequency steps subject to a total mass constraint. The frequency response governing equation is solved using OptiStruct modal frequency response analysis.

$$\begin{aligned} &\text{minimize:} && \sum_{n}\sum_{\omega} ERP_{\omega n}\left(\underset{\sim}{x}\right) \\ &\text{subject to:} && \underset{\sim}{M}\ddot{\underset{\sim}{u}} + \underset{\sim}{C}\dot{\underset{\sim}{u}} + \underset{\sim}{K}\underset{\sim}{u} = \underset{\sim}{f}_n e^{i\omega t} \\ & && \text{mass} \le 8.8 \text{ kg} \\ & && 1.270\text{mm} \le x_e \le 2.032\text{mm} \\ & && \forall e \text{ skin elements}, \forall \omega \text{ frequencies}, \forall n \text{ loads} \end{aligned} \tag{5}$$

The thickness design variables were restricted such that each bay (the area between the stringers and frames) on the panel are identical to one another. Each bay was also restricted to a symmetric pattern about two axes. These design constraints were simultaneously applied using a master and slave definition shown in Fig. 3. This implementation results in only a quarter of a one bay with independent design variables, and all other element thicknesses linked to the master design variable values. No other manufacturing constraints are needed as the chemical-milling process can produce complex geometry with minimal added cost.

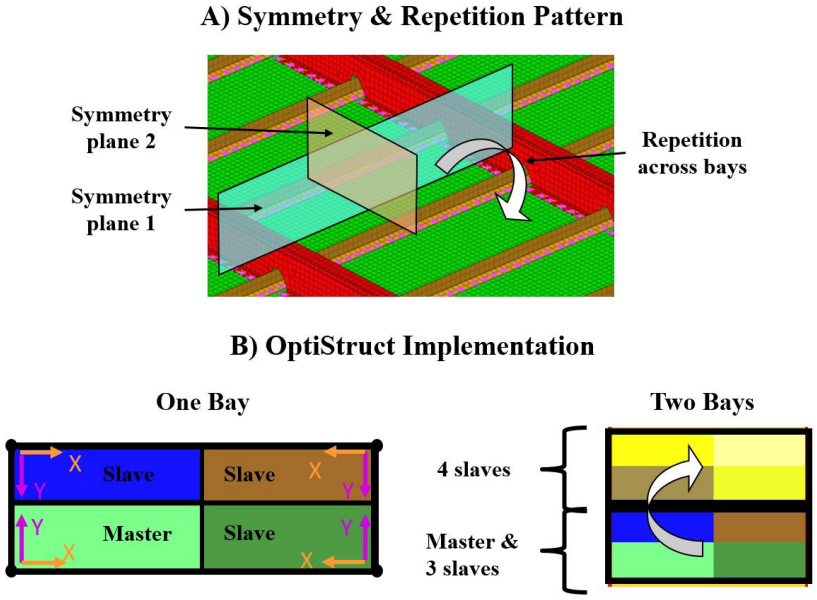

Fig. 3 Symmetry and pattern repetition design constraints for chemical-milled pockets.

III. Results

First, sound power and ERP were analyzed for a stiffened panel with a uniform skin thickness to compare the ideal response value with the response used during optimization. Next, free-size optimization of the skin panel was conducted with an ERP objective function. Finally, the optimized results were interpreted and compared to the baseline geometry and other chemical-milled pocket designs. All models and optimization were completed using Altair OptiStruct running on a Windows PC (18 cores @ 2.6 GHz, 128 GB RAM) resulting in run times of approximately 45 minutes for analysis and 6 hours for optimization.

A. Analysis

A plot of A-weighted ERP and sound power for the stiffened panel with a 1.27 mm uniform thickness for the random loading in Fig. 2 B) is shown in Fig. 4. It is evident that ERP overestimates sound power for the entire

frequency spectrum, which is expected based on previous research [18] and radiation efficiency theory [19] as the applied frequencies are below the plate's critical frequency (calculated to be approximately 10 kHz). The other conclusion to be drawn from this plot is that all peaks in ERP do not correspond to peaks in sound power, due to the cancellation effect described by Fahy and Gardonio [19]. For example, the second peak in ERP at 73 Hz (indicated by the vertical line) occurs at the mode 2-1, in which a significant cancellation effect occurs, resulting in no peak in the sound power curve. Therefore, an ERP reduction of this peak may not be associated with a reduction in sound power.

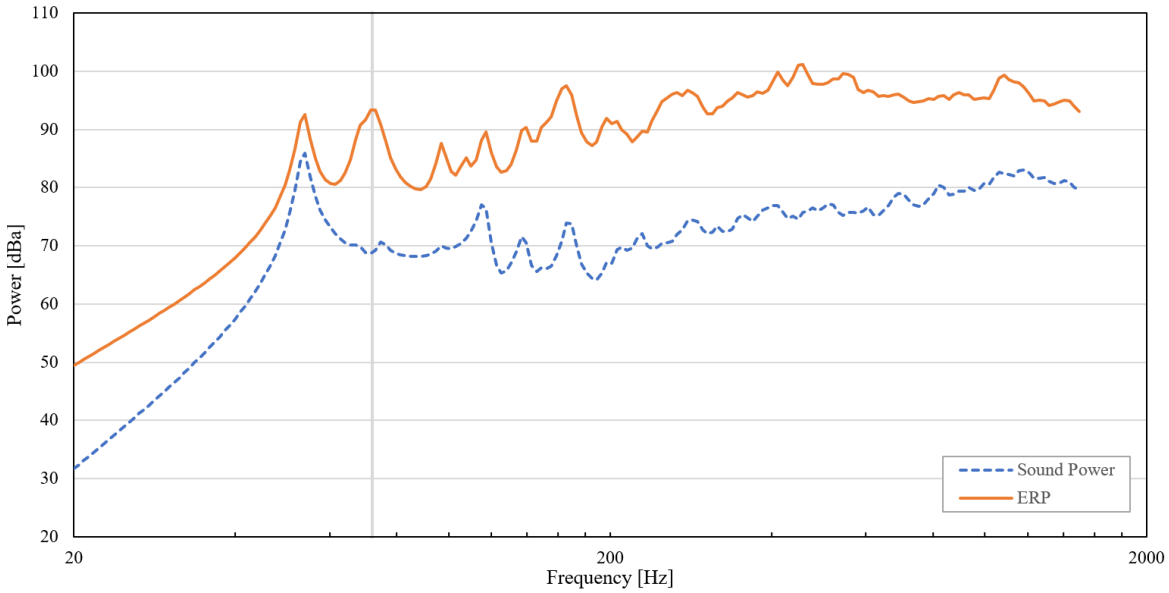

Fig. 4 A-weighted ERP and sound power of a uniform thickness panel

B. Optimization

The ERP optimization was conducted using the distributed loads in Fig. 2 A with a mass limit of 8.8 kg, corresponding to the mass of a stiffened panel with a 1.44 mm uniform plate. The free-size optimization converged after 8 iterations, producing the element thickness distribution shown in Fig. 5. The optimization resulted in a 120 mm x 55 mm rectangular section of maximum thickness in the center of each bay, with adjacent areas about 1.6mm thick. There were localized increases in thickness at the intersection of the stringers and frames, however these are not manufacturable as the stiffeners must be attached to a uniform surface on the plate. It is important to note that the variable thickness design produced by the optimization cannot be manufactured by chemical-milling as only discrete thicknesses can be produced. A design with multiple discrete thicknesses (requiring multiple chemical baths) may not be feasible from a cost perspective. Therefore, this design must be interpreted into a design that is more realistic before assessing sound power.

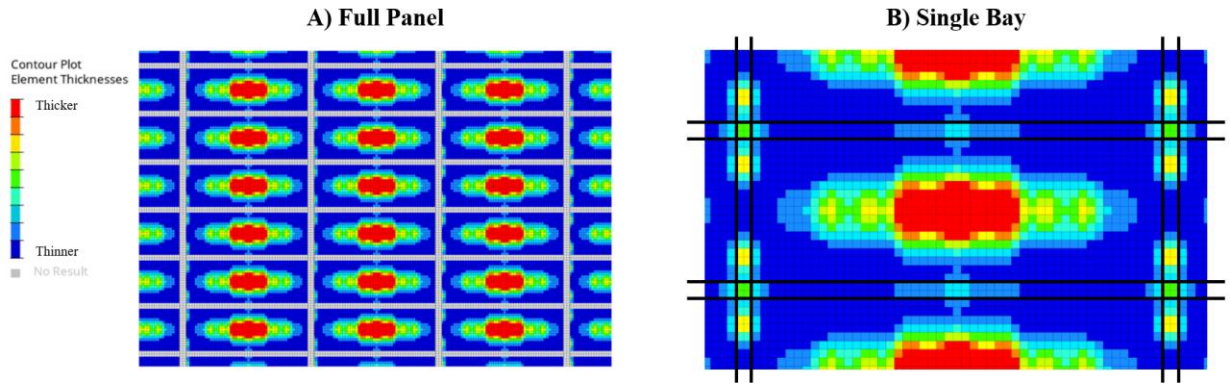

Fig. 5 Free-size optimization results of chemical-milled pockets.

The optimization reduced the ERP objective function by 13% (or 0.53 dB) compared to the uniform thickness stiffened plate of the same mass. The objective and constraint function history are shown in Fig. 6. Note that the value in Watts of the ERP objective function is not physically meaningful as it is a summation over all frequencies and all loading locations, for unit loads.

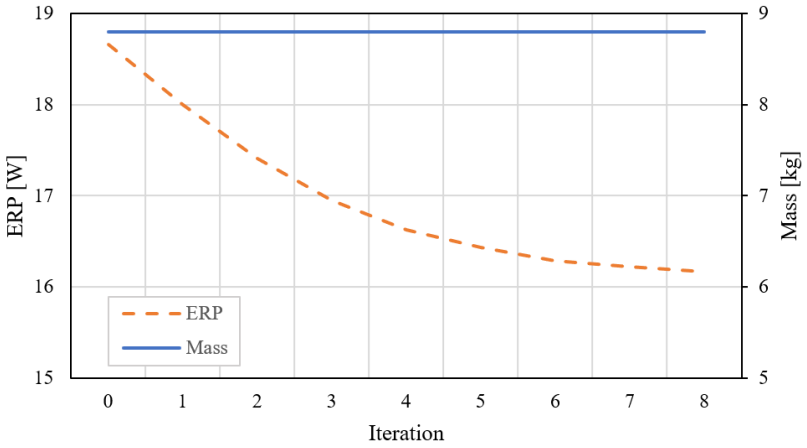

Fig. 6: Optimization history of stiffened panel.

The ERP frequency response plot of the original and optimized plate in Fig. 7 demonstrates near identical performance below 120 Hz and decreases in ERP across the spectrum of 120 – 1500 Hz. ERP in Fig. 7 is plotted in units of mW in logarithmic scale without A-weighting to demonstrate how ERP is interpreted by the optimization algorithm.

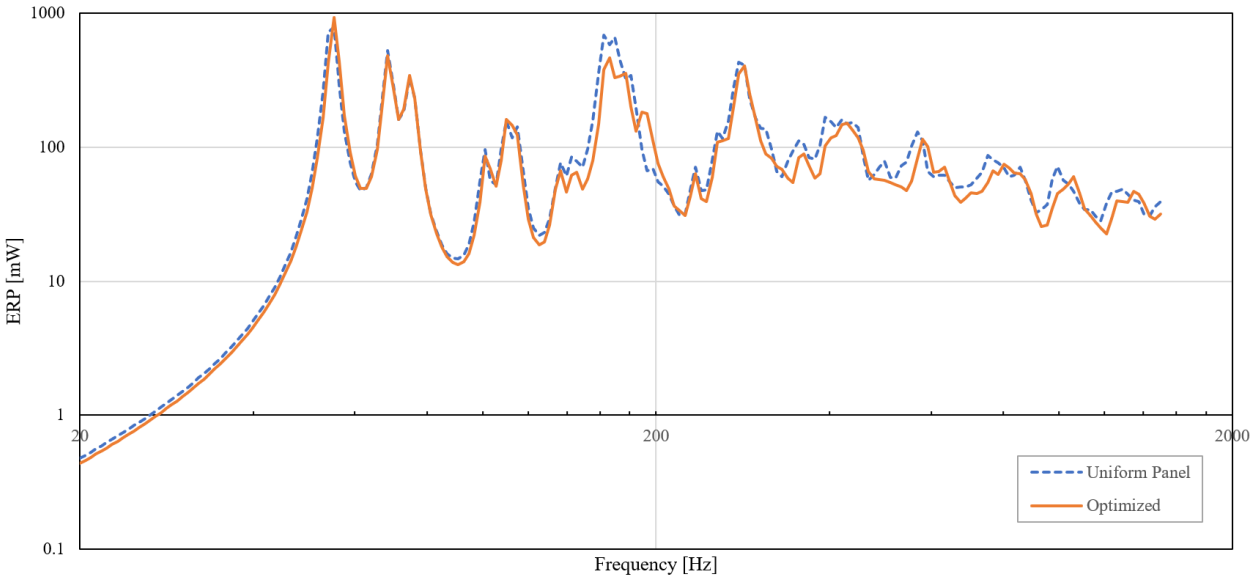

Fig. 7 ERP frequency response of optimized and original (uniform panel).

C. Design Comparison

The free-size optimization results from Fig. 5 were interpreted into the manufacturable pocket design shown in Fig. 8 F. This chemical-milled design has two discrete thicknesses, with the green elements representing the full thickness plate and dark blue elements representing the chemical milled portion. The optimized design was compared to other chemical-milled designs in Fig. 8 A - D. Finally, the design was compared with a uniform thickness plate in Fig. 8 E. All designs have an equivalent mass of 8.8 kg and were analyzed for the same 100 random loads from Fig. 2 B. These images show a single bay design with transparent stringers and frames.

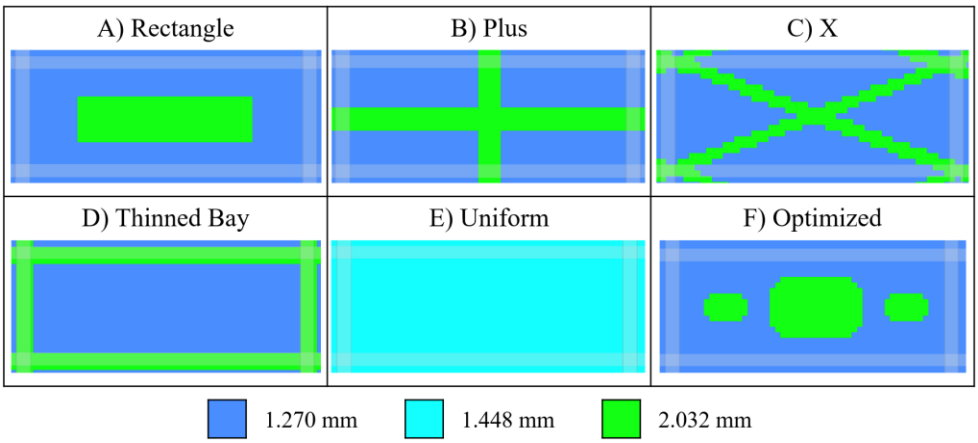

Fig. 8 Chemical-milled pocket designs compared in sound power analysis.

The sound power generated by each design is plotted in Fig. 9, with a difference of 0.81 dB calculated between the models with the highest and lowest sound power (design D at 76.30 dBa and design F at 75.49 dBa, respectively). This decibel range represents an approximate 6% difference in loudness, which may not be significant as the general rule of thumb is that differences less than 1 dB are not noticeable to the human ear. While the optimized model F performed best, it has functionally identical sound power as designs A, B, C, and E. On the other hand, design D performed worse than all other models. An important takeaway from this comparison is that fully thinning the entire bay with chemical milling has a negative impact of sound power that is approaching a perceptible range. Instead of using chemical milling, switching to a uniform plate with a lower thickness would reduce mass without affecting sound power.

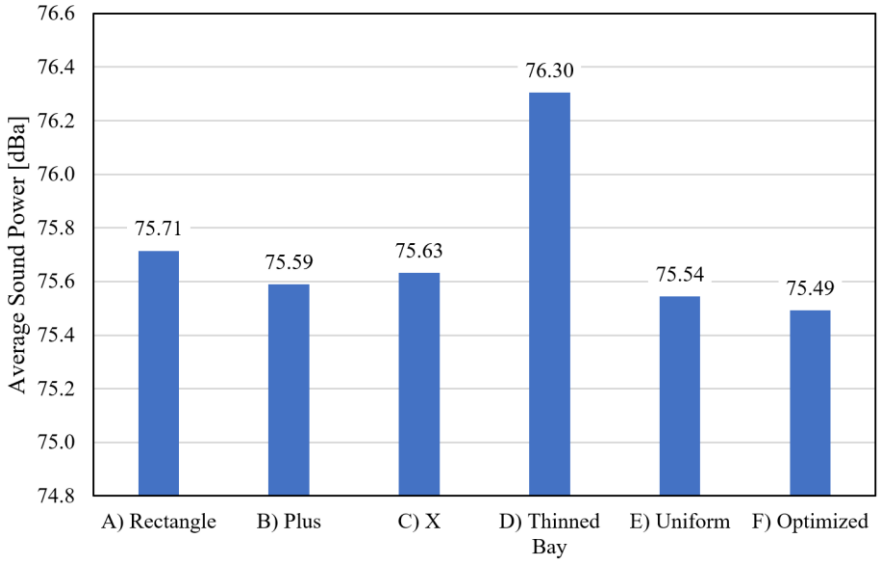

Fig. 9 Sound power results for all chemical-milled pocket designs

It should also be noted that the sound power improvements relative to a uniform plate calculated in ERP during optimization (about 0.53 dB) did not carry over to the sound power domain, as the difference between the uniform thickness and optimized designs was only 0.05 dB. This may be due to the previously discussed differences between sound power and ERP or could be due to the simplifications made when interpreting the design from the continuous density field to a discrete, manufacturable design.

A comparison of sound power across octave bands is shown in Fig. 10 for the conventional chemical-milling design, a uniform plate, and the optimized design. In all designs, the 1000 Hz octave band contributes the most and the 31.5 Hz octave band contributes the least towards overall sound power. Larger improvements in sound power were achieved when focusing on localized octave bands, whereas changes were more likely to average out when considering

the full frequency range. For example, a 1.1 dB reduction was achieved by the optimized design relative to the thinned pocket design in the 63 Hz and 500 Hz octave bands. Interestingly, the optimized design had a 4.4 dB higher sound power in the lowest octave band, but this band contributes very little to the full frequency result as the sound power in this octave band is much lower.

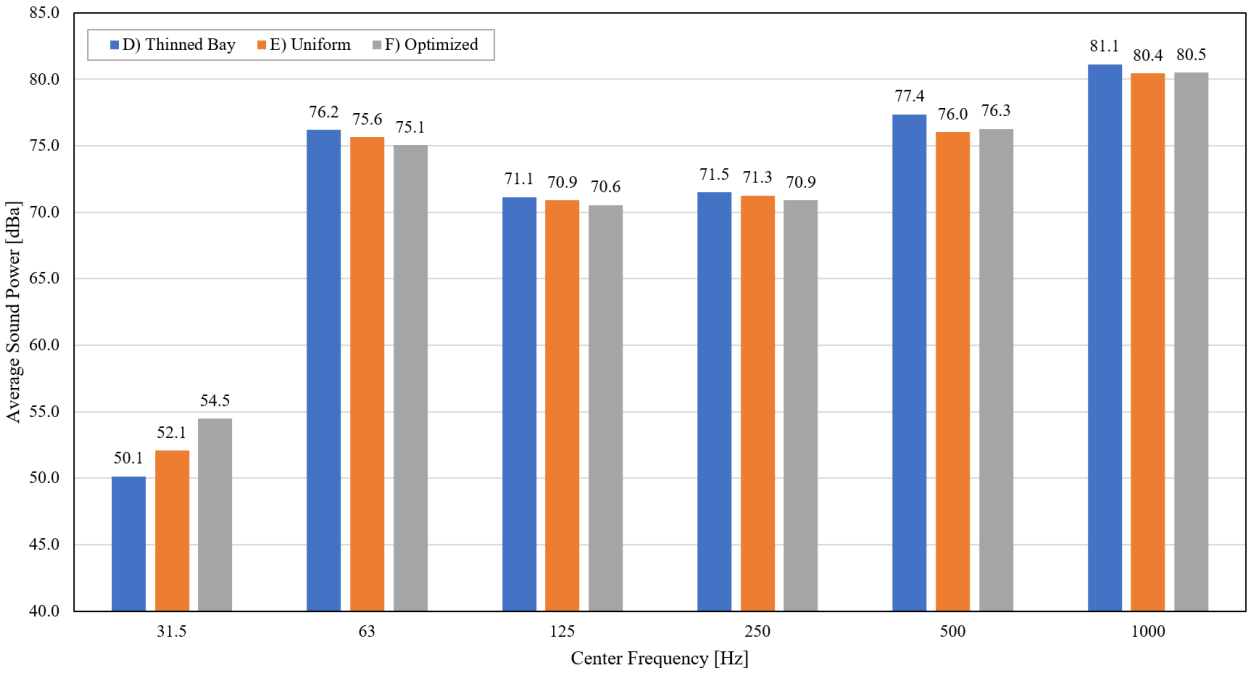

Fig. 10 Sound power results across octave bands for designs D - F

IV. Conclusions

Equivalent radiated power is a simple approximation for sound power that is calculated from the normal velocities of a vibrating surface and can be output from a frequency response analysis in finite element solvers. However, the ERP calculation ignores acoustic short circuits, which reduces accuracy when compared to sound power calculated with a Rayleigh integral. A comparison of ERP and sound power for a stiffened panel model demonstrated that ERP overestimates sound power for the presented frequency range, and that some peaks in ERP did not correspond to peaks in sound power.

This work presented a free-size optimization approach for minimizing ERP, a more accessible objective function compared to the desired objective of minimizing sound power. This technique was applied to the design of chemical-milled pockets for a stiffened panel model. The optimization reduced ERP by 13% when measured in Watts compared to a uniform thickness stiffened plate. The optimization results were interpreted into a manufacturable chemical-milled design, which was compared against five other models for sound power. The optimized design achieved the lowest sound power but was comparable to many other pocket designs, while the thinned bay design performed the worst. Across all designs, the largest difference in sound power was 0.81 dB, which may not be perceptible to the human ear. The ERP optimization successfully generated a unique design that minimized sound power relative to the designs explored, however only a small reduction in sound power was achieved.

In the future, the ERP optimization methodology will be extended to other stiffened panel design variables, including stiffener spacing and stiffener cross-section, to determine if more significant reductions in sound power can be achieved. Other criteria such as stiffness, stress, and cost should ultimately be considered to investigate potential trade-offs between acoustic and structural performance determining the optimal design. The loading cases could be improved to more accurately represent the acoustics excitation experienced by the aircraft during flight. While the averaged sound power response of 100 randomly placed unit loads does not have any bias to a particular location, it only excites a localized point in each load case. Implementing a turbulent boundary layer excitation, or an equivalent approximation, would improve the accuracy of the results. In general, more study is needed to determine how changes in structural design affect sound power and to understand the fundamental physical principles that govern the relationship between the structure and the sound power generated.

Acknowledgments

This research was funded by Natural Sciences and Engineering Research Council of Canada (NSERC) and industry partner Bombardier Inc. Technical advice and guidance were gratefully received from Andrew Wareing, Manuel Etchessahar, Stephen Colavincenzo, and Sehrish Waseem. This project would not have been possible without their knowledge, continuous support, and feedback.

References

[1] Mixson, J. S., and Powell, C. A., "Review of Recent Research on Interior Noise of Propeller Aircraft," *Journal of Aircraft*, Vol. 22, No. 11, 1985, pp. 931-949.
doi: 10.2514/3.45229

[2] Bouwens, J., Hiemstra-van Mastrigt, S., and Vink, P., "Ranking of Human Senses in Relation to Different In-flight Activities Contributing to the Comfort Experience of Airplane Passengers," *International Journal of Aviation Aeronautics and Aerospace*, Vol. 5, No. 2, 2018.
doi: 10.15394/ijaaa.2018.1228

[3] Mellert, V., Baumann, I., Freese, N., and Weber, R., "Impact of sound and vibration on health, travel comfort and performance of flight attendants and pilots," *Aerospace Science and Technology*, Vol. 12, No. 1, Jan. 2008, pp. 18-25.
doi: 10.1016/j.ast.2007.10.009

[4] Wilby, J. F., "Aircraft interior noise," *Journal of Sound and Vibration*, Vol. 190, No. 3, Feb. 1996, pp. 545-564.
doi: 10.1006/jsvi.1996.0078

[5] SobieszczanskiSobieski, J., and Haftka, R. T., "Multidisciplinary aerospace design optimization: survey of recent developments," *Structural Optimization*, Vol. 14, No. 1, Aug. 1997, pp. 1-23.
doi: 10.1007/bf01197554

[6] Zhu, J. H., Zhang, W. H., and Xia, L., "Topology Optimization in Aircraft and Aerospace Structures Design," *Archives of Computational Methods in Engineering*, Vol. 23, No. 4, Dec. 2016, pp. 595-622.
doi: 10.1007/s11831-015-9151-2

[7] Roper, S. W. K., Lee, H., Huh, M., and Kim, I. Y., "Simultaneous isotropic and anisotropic multi-material topology optimization for conceptual-level design of aerospace components," *Structural and Multidisciplinary Optimization*, Vol. 64, No. 1, Jul. 2021, pp. 441-456.
doi: 10.1007/s00158-021-02893-4

[8] Munroe, E., Bohrer, R., Chishty, W. A., and Kim, I. Y., "Structural design of a morphing serpentine inlet using a multi-material topology optimization methodology," *Structural and Multidisciplinary Optimization*, Vol. 64, No. 1, Jul. 2021, pp. 389-422.
doi: 10.1007/s00158-021-02885-4

[9] Hardman, A., Crispo, L., Sirola, T., Ann, J., Lee, J., Song, J. H., and Kim, I. Y., "Structural Design Optimization for CFRP in a Personal Aerial Vehicle," *AIAA Aviation 2021 Forum*, 2021.

[10] Marburg, S., "Developments in structural-acoustic optimization for passive noise control," *Archives of Computational Methods in Engineering*, Vol. 9, No. 4, 2002, pp. 291-370.
doi: 10.1007/bf03041465

[11] Lamancusa, J. S., "Numerical Optimization Techniques for Structural-Acoustic Design of Rectangular Panels," *Computers & Structures*, Vol. 48, No. 4, Aug. 1993, pp. 661-675.
doi: 10.1016/0045-7949(93)90260-k

[12] Cunefare, K. A., Crane, S. P., Engelstad, S. P., and Powell, E. A., "Design minimization of noise in stiffened cylinders due to tonal external excitation," *Journal of Aircraft*, Vol. 36, No. 3, May-Jun. 1999, pp. 563-570.
doi: 10.2514/2.2471

[13] Du, J. B., and Olhoff, N., "Minimization of sound radiation from vibrating bi-material structures using topology optimization," *Structural and Multidisciplinary Optimization*, Vol. 33, No. 4-5, Apr. 2007, pp. 305-321.
doi: 10.1007/s00158-006-0088-9

[14] Warwick, B. T., Mechefske, C. K., and Kim, I. Y., "Topology optimization of a pre-stiffened aircraft bulkhead," *Structural and Multidisciplinary Optimization*, Vol. 60, No. 4, Oct. 2019, pp. 1667-1685.
doi: 10.1007/s00158-019-02284-w

[15] Warwick, B. T., Mechefske, C. K., and Kim, I. Y., "Natural Frequency Based Topology Optimization of an Aircraft Engine Support Frame," *ASME 2020 International Design Engineering Technical Conferences and Computers and Information in Engineering Conference*, Vol. 7, 2020.

[16] Altair, "Altair OptiStruct 2019 User Guide," Altair Engineeering Inc., 2019

[17] Kim, H. G., Nerse, C., and Wang, S., "Topography optimization of an enclosure panel for low-frequency noise and vibration reduction using the equivalent radiated power approach," *Materials & Design*, Vol. 183, Dec. 2019.
doi: 10.1016/j.matdes.2019.108125

[18] Fritze, D., Marburg, S., and Hardtke, H. J., "Estimation of Radiated Sound Power: A Case Study on Common Approximation Methods," *Acta Acustica United with Acustica*, Vol. 95, No. 5, Sep-Oct. 2009, pp. 833-842.
doi: 10.3813/aaa.918214

[19] Fahy, F., and Gardonio, P., *Sound and Structural Vibration (Second Edition)*, Academic Press, Oxford, pp. 135-195
[20] Luegmair, M., and Munch, H., "Advanced Equivalent Radiated Power (ERP) Calculation for Early Vibro-Acoustic Product Optimization," *22nd International Congress on Sound and Vibration (ICSV)*, Florence, Italy, 2015.
[21] Chandregowda, S., and Reddy, G. R. C., "Evaluation of Fastener Stiffness Modelling Methods for Aircraft Structural Joints," *Advances in Mechanical Design, Materials and Manufacture*, Amer Inst Physics, India, 2018.
[22] Etchessahar, M., and Gagliardini, L., "Quantification of structural damping of a multi-layered windshield at low and medium frequencies," *The Journal of the Acoustical Society of America*, Vol. 123, No. 5, 2008, pp. 3534-3534. doi: 10.1121/1.2934499